Stop A1/1

UNTERSBERG SECTION NEAR FÜRSTENBRUNN

Hans Egger, Fred Rögl

Topics:
Paleocene/Eocene-boundary and lower Eocene bentonites in bathyal marlstone and claystone

Tectonic unit:
Northern Calcareous Alps

Lithostratigraphic units:
Gosau Group, Nierental Formation

Chronostratigraphic units:
Upper Paleocene to Lower Eocene

Biostratigraphic units:
Calcareous Nannoplankton Zones NP9 and NP10a; Planktonic Foraminifera Zones P5 to E3

Location:
Tributary of the Kühlbach near Fürstenbrunn

Coordinates:
47° 44′ 19″ N, 012° 59′ 04″ E

References:
Egger et al. (2005), Egger & Brückl (2006), Hillebrandt (1962), Hagn et al. (1981)

Outcrop 1a: Paleocene/Eocene-boundary

From the bus stop it is a 10 minutes downhill walk through the forest (no trail!) to reach the outcrops, which are located along the course of a creek. Estimated duration of the stop is 1.5 hours.

The Paleogene deposits of the Untersberg region were examined by von Hillebrandt (1962 and in Hagn et al., 1981. The more than 1000 m thick Paleogene succession of the Untersberg area consists predominantly of marlstone displaying carbonate contents between 40 wt% and 50 wt%. Abundant planktonic foraminifera and calcareous nannoplankton are the main source of the carbonate. Von Hillebrandt (1962) already recognized the importance of the benthic foraminiferal extinction at the end of the Paleocene and Egger et al. (2005) re-examined this outcrop. However, at that time the exposure was worse and only part of the CIE-interval was outcropping. In 2010, a flood event due to torrential rain significantly improved the outcrop situation and revealed also minor faults along the dipping planes.

Figure A1.3 ▲
Photograph of the outcrop 1a at Untersberg showing the grey and red claystone of the CIE-interval

At the base of the new outcrop (Fig. A1.3) grey marlstone shows a sharp contact to grey claystone, which is overlain by red claystone. The claystone at the P/E-boundary indicates a deposition below the CCD. Excluding the carbonate content, the mean percentages of the siliciclastic components are almost identical below and above the CIE−interval: 16.3 % quartz and feldspar and 83.7 % clay minerals from the interval above the CIE and 16.6 % quartz and feldspar and 83.4 % clayminerals below the CIE. Within the CIE−interval, however, the mean percentage of quartz and feldspar is 24.8 %, which is equivalent to an increase of 49 % in relation to the other parts of the section.

The clay mineral assemblage at Untersberg is strongly dominated by smectite (72 wt%), followed by illite (18 wt%), kaolinite (6 wt%) and chlorite (4 wt%). The abundance of smectite throughout the studied section, together with the absence of mixed−layers, indicates that the rocks of the Untersberg section were not affected by deep−burial diagenesis. Consequently, diagenetic effects on the composition of clay mineral assemblages can be ruled out.

At its top, this claystone displays a gradual increase in calcium carbonate contents (Fig. A1.5) already documented by Egger et al. (2005). This transition zone to the overlying grey marlstone indicates a deposition within the lysocline, which is the water depth where carbonate dissolution rates are greatly accelerated (Berger, 1970). The gradual change of carbonate content within the transition zones suggests a slow shift of the level of the lysocline and CCD at the end of the CIE and has been described also from sections elsewhere (Zachos et al., 2005).

Calcareous nannoplankton

Calcareous nannofossils were found in the marlstone and in the transition zones (marly claystone) between the marlstone and the shale. They are abundant (> 30 specimens per field of view) in the samples from the marlstone, whereas their abundance is low (< 10 specimens per field of view) in the samples from the transition zones. The preservation of nannofossils is moderate in the marlstone and poor in the transition zone according to the classification of Steinmetz (1979). In the moderately preserved sam-

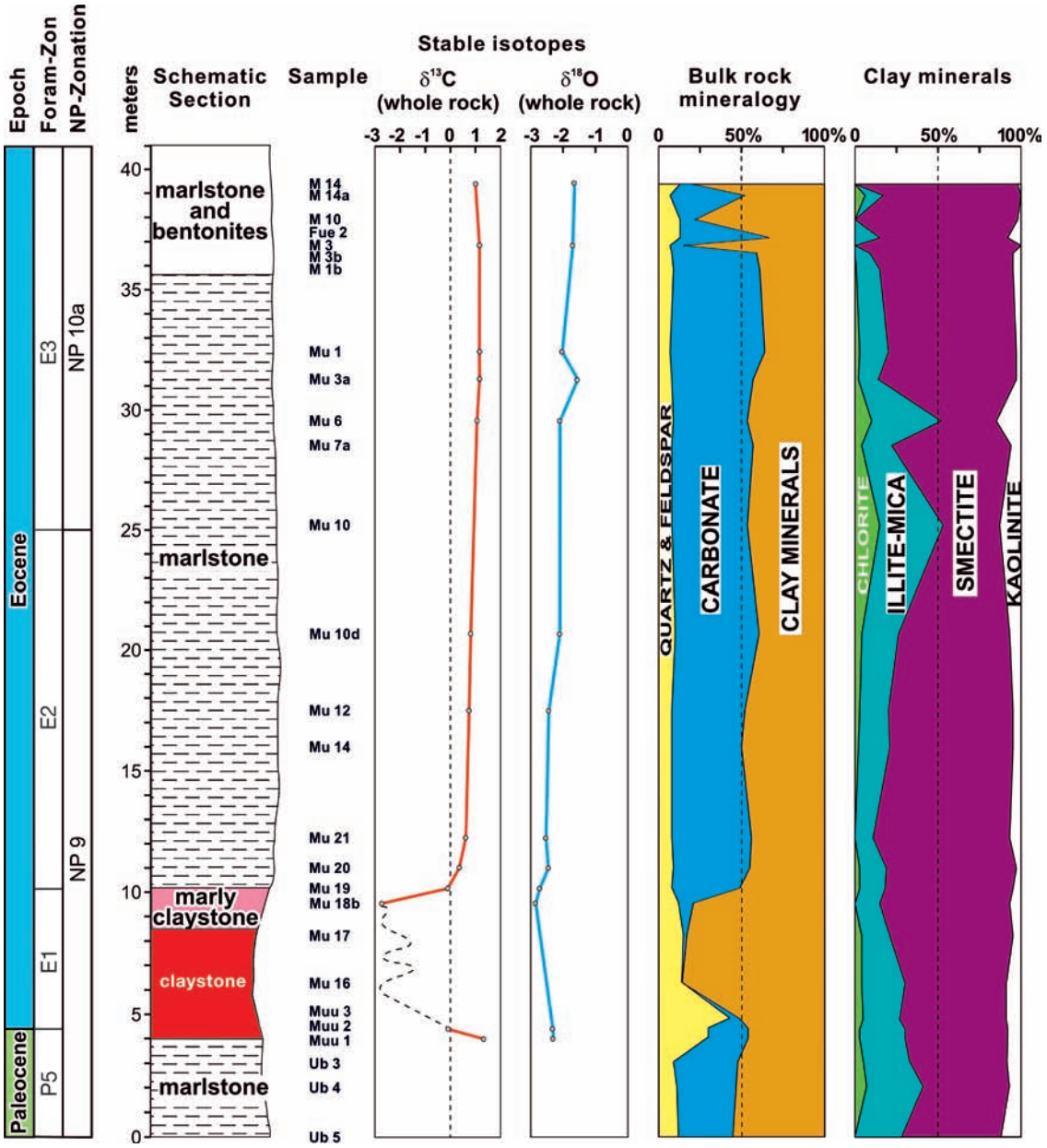

Figure A1.4 ▲
Carbon isotope values, bulk rock mineralogy, and composition of clay mineral assemblages across the Paleocene–Eocene boundary.

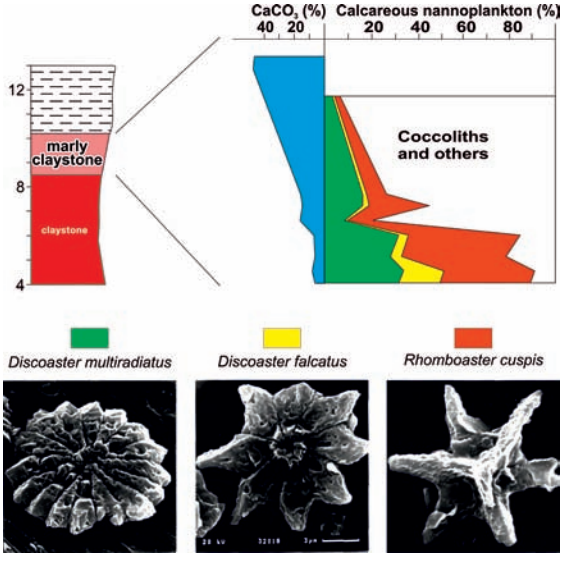

Figure A1.5 ◄
Percentages of *Discoaster multiradiatus*, *Discoaster falcatus*, and *Rhomboaster cuspis* in the calcareous nannoplankton assemblages and calcium carbonate percentages at the top of the CIE–interval (scale bar represents 3 µm and is valid for all photographs).

ples the majority of the specimens are slightly etched but all taxa can be easily identified and diversity is about 16 species per sample on average. In the poorly preserved samples, the majority of specimens are deeply etched, identification of taxa is difficult and the diversity is only about 6 species per sample.

Reworked specimens are present in the marlstone samples, with rare Cretaceous species appearing (less than 1% of the nannofossil assemblage). Reworking has affected mainly Upper Cretaceous deposits, indicated by the occurrences of *Micula decussata*, *Prediscosphaera cretacea*, *Lucianorhabdus cayeuxii*, *Broinsonia parca*, *Ceratolithoides aculeus*, *Uniplanarius trifidus* and *Arkhangelskiella cymbiformis*. In one sample (M3b) typical Lower Cretaceous species (*Micrantolithus hoschulzii* and *Nannoconus steinmannii*) were also found. However, the relatively common *Watznaueria barnesae* specimens in most samples may in part also originate from Lower Cretaceous deposits, as this species is abundant throughout the entire Cretaceous.

The Paleogene nannoflora is dominated by *Coccolithus pelagicus*, which usually accounts for about 90% of the nannoplankton assemblages, with the exception of the poorly preserved assemblages of the CIE−interval. *Discoaster multiradiatus,* the zonal marker of NP9, is another common species and the only species occurring in all samples. Species of the stratigraphically important genus *Fasciculithus* are rare in the Untersberg section, except in the samples from below the CIE. *Scapholithus apertus* is the only species which becomes extinct at the Palaeocene−Eocene boundary of the Untersberg section.

The first specimens of the genus *Rhomboaster* occur just below the base of the CIE. There, short−armed specimens of *Rhomboaster cuspis* are exceedingly rare. In contrast, in the samples from the top of the CIE−interval *Rhomboaster cuspis* is the dominant species (up to 49% of the assemblages) followed by *Discoaster multiradiatus* and *Discoaster falcatus*. Rare specimens of *Discoaster araneus* occur. In other Tethyan sections *Discoaster anartios* (Bybell and Self−Trail, 1994) co−occurs with *Discoaster araneus*; however, this species has not been found at Untersberg. Coccoliths are absent or extremely rare in this CIE−assemblage.

The unusual composition of the nannoplankton assemblage of the marly claystone at the top of the CIE−interval is an effect of carbonate dissolution because, synchronously with increasing carbonate content, the calcareous nannoplankton shows better preservation and a higher diversity (Fig. A1.5). The species diversity in nannoplankton assemblages is, to large extent, controlled by selective dissolution of skeletal elements. Bukry (1971) recognized that *Discoaster* is the most dissolution−resistant genus among the Cenozoic genera, followed by the genus *Coccolithus*. At Untersberg, the high percentages of *Rhomboaster* in the transition zone assemblages are most probably an effect of selective dissolution, indicating that *Rhomboaster* has a similar resistance to dissolution as *Discoaster.*

Foraminifera

Planktonic and benthic foraminifera are very abundant in most of the studied samples, although, as a result of carbonate dissolution, their preservation is poor across the CIE-interval. There, the assemblages are strongly dominated by agglutinating taxa. A specific determination was often difficult to make as many planktonic foraminifera specimens are corroded or deformed. For this reason no quantitative analysis of the foraminifera fauna was conducted, despite recording 191 different taxa in 19 samples, excluding species reworked from the Upper Cretaceous and Lower Paleocene (mainly Danian). The distribution of planktonic foraminifera is given in Tab. 1. The planktonic foraminiferal biozonation follows the criteria of Berggren & Pearson (2005).

Zone P5 (*Morozovella velascoensis* Partial-range Zone), the uppermost zone in the Paleocene, is defined by the highest occurrence (HO) of *Globanomalina pseudomenardii* and the lowest occurrence (LO) of *Acarinina sibaiyaensis*. At Untersberg, only reworked specimens of *G. pseudomenardii* occur, wheras *A. sibaiyaensis* is absent and has not been found in Eastern Alpine sections till now. The assignment of the lowermost part of the studied section to Zone P5 is due to the occurrence of *Morozovella subbotinae*, which has a stratigraphic range from Zone P5 to Zone E5. In this part of the section also *M. aequa* and *M. gracilis* occur.

Due to the scarcity of planktonic foraminifera in the claystone of the CIE-interval no zonal attribution was possible. In the overlying marlstone (sample MU 19/97) *Pseudohastigerina wilcoxensis* was found, indicating Zone E2 (*Pseudohastigerina wilcoxensis/Morozovella velascoensis* Concurrent-range Zone). This zone is defined as the interval between the LO of *P. wilcoxensis* and the HO of *M. velascoensis*.

UNTERSBERG KÜHLBACHGRABEN Planktonic Foraminifera	Ub 5/2003	Ub 4/2003	Ub 3/2003	Untersberg 1/10	MUU 2/99	MUU 3/99	Untersberg 2/10	Untersberg 2B/10	Untersberg 3/10	MU 17/97	Mu 18a/97	MU 18d/96	MU 19/97	MU 20/97	MU 21/97	MU 14/97	MU 12/97	MU 10d/97	MU 10/97	below MU 7/97	MU 6/97	below M 1	above M 14	Zonal Ranges acc. Olsson et al. 1999, Pearson et al. 2006
Acarinina coalingensis (CUSHMAN & HANNA)	x	cf.		x											x	x	x	x	cf.	x	x	x	x	P4c-E7
Acarinina mckannai (WHITE)	x	x	x	x			x				x		x	x	x	cf.	cf.	cf.	x	x		x	x	P4a-b
Acarinina nitida (MARTIN)	x	x	x	x		x	x		x		x		x	x	x	x	x	x	x	x	x	x	x	P4
Acarinina soldadoensis (BRÖNNIMANN)	x	x		x			x										x	cf.	x	x	x	x	x	P4c-E7
Acarinina subsphaerica (SUBBOTINA)	cf.	cf.		x		x	x						x				x				x			P4-E3
Subbotina cancellata (BLOW)	cf.	x	x	x										x	x		cf.					cf.		P2-P4b
Subbotina triangularis (WHITE)	x	x	x	x		x	x	x					x	x	x	x	x	x	x	x	x	x		P2-P5
Subbotina triloculinoides (PLUMMER)	x	x	x	x		cf.	x			cf.	cf.							x						P1b-P4a
Subbotina velascoensis (CUSHMAN)	x	x	x	x			x	x					x	x	x	x	x	x	x	x	x	x	x	P3b-E2
Morozovella acuta (TOULMIN)	x																							P4b-E2
Morozovella aequa (CUSHMAN & RENZ)	x	x	x	x									x	x	x		x		x	x	x	x		P4c-E5
Morozovella gracilis (BOLLI)	cf.		x	cf.			x						x	x	x			x			x	x	x	P5-E5
Morozovella occlusa (LOEBLICH & TAPPAN)	x	x	x						x				x	x			x		x					P4-P5
Morozovella subbotinae (MOROZOVA)	x	x	x	x		x								x	x	x	x	x	x	x	x	x	x	P5-E5
Morozovella velascoensis (CUSHMAN)	x	x	x	x									cf.	cf.	x	x	x	x			r			P3b-E2
Globanomalina pseudomenardii (BOLLI)	x		cf.	x	agglutinated foraminifera							agglutinated foraminifera												reworked
Praemurica spp.	x	x		x																				reworked
Parvularugoglobigerina sp.		x	x																					reworked
Parasubbotina pseudobulloides (PLUMMER)		x		x																				reworked
Parasubbotina varianta (SUBBOTINA)		x	x	x																				P1c-E10
Acarinina strabocella (LOEBLICH & TAPPAN		x	x																					reworked
Igorina albeari (CUSHMAN & BERMUDEZ)		x	x	x																				reworked
Morozovella pasionensis (BERMUDEZ)			x	x																				P3b-E2
Globanomalina planocompressa (PLUMMER)				x																				reworked
Globanomalina imitata (SUBBOTINA)				x																				reworked
Morozovella marginodentata (SUBBOTINA)				x			x												x	x		x	x	P5-E5
Subbotina incisa (HILLEBRANDT)							x						x	x	x	x	x	x		x		cf.	cf.	
Morozovella angulata (WHITE)													cf.											P3-P4a
Morozovella apanthesma (LOEBLICH & TAPPAN)													x		x								x	P3b-P4
Acarinina quetra (BOLLI)											x		x		x					x	cf.	x	x	E3-E6
Globanomalina planoconica (SUBBOTINA)													x		x				x		x	x	x	P4c-E6
Pseudohastigerina wilcoxensis (CUSHMAN & PONTON)													x						x					E2-E10
Globanomalina chapmani (PARR)															x			x						P3b-P5
Igorina broedermanni (CUSHMAN & BERMUDEZ)															cf.						x		cf.	E1-E9
Acarinina pentacamerata (SUBBOTINA)															cf.			x				x	x	
Acarinina pseudotopilensis SUBBOTINA																x	x					x		E1-E7
Subbotina linaperta (FINLAY)																					x	x		
Parasubbotina inaequispira (SUBBOTINA)																						x	x	E1-E8
Acarinina wilcoxensis (CUSHMAN & PONTON)																						x	x	P5-E5
Planorotalites pseudoscitula (GLAESSNER)																						x	x	P5-E7
Igorina salisburgensis (GOHRBANDT)																						x	x	
Morozovella edgari PREMOLI SILVA & BOLLI																						x	x	E2-E3
Upper Cretaceous	x	x		x	x	x							x	x	x	x	x	x	x	x	x		x	reworked
Planktonic Foraminfera Zones	P5					E1 ?							E2						E3					

Table 1 ▲
Planctonic foraminifera of the Untersberg section

M. velascoensis has its HO in sample MU 10d/97. Further up-section, rare specimens of this species (sample MU 6/97) are considered to be reworked. The LO of *Morozovella edgari* is used to assign the highest part of the section to Zone E3 (*Morozovella marginodentata* Partial-range Zone). This zone is defined by the HO of *M. velascoensis* and the LO of *M. formosa*, however, the latter species does not occur in our samples.

The distribution of calcareous benthic foraminifera is similar to those of other deep−water sections (see Thomas, 1998, for a review). *Gavelinella* cf. *beccariiformis* has its HO at the onset of the CIE. The post−extinction calcareous benthic foraminifera assemblages are dominated by *Nuttalides truempyii* (very small specimens), *Abyssamina poagi, Anomalinoides nobilis, A. praeacutus, Oridorsalis spp*. and a number of pleurostomellids (e.g. *Ellipsoglandulina*, *Ellipsoidella, Ellipsopolymorphina*, *Nodosarella*, *Pleurostomella*). This assemblage is typical of lower bathyal to abyssal environments (van Morkhoven et al., 1986). For example, *Abyssamina poagi* occurs between 1700 m and 4000 m depth, and *Oridorsalis lotus* indicates a depth of between 800 m and 1900 m. This suggests a palaeodepth of about 2000 m (lower bathyal) for the deposition of Untersberg section.

The agglutinating foraminiferal fauna consists of 68 species, 25 of which (37 % of the entire fauna) occur exclusively at the base of the succession and end within the CIE−interval. These species are *Ammodiscus cretaceus, Aschemocella carpathica, A. grandis, Bathysiphon? annulatus, Caudammina arenacea, C. excelsa, C. ovulum, Dorothia beloides, Glomospira diffundens, G. glomerata, G. serpens, Haplophragmoides walteri, Hormosinella distans, Hyperammina lineariformis, Karrerulina horrida, Psammotodendron? gvidoensis, Psammosiphonella sp., Remesella varians, Rzehakina fissistomata, Saccamina grzybowskii, Silicobathysiphon sp., Subrheophax pseudoscalaris, S. splendidus, Trochamminoides folius,* and *T. subcoronatus.* In the upper part of the succession the typical assemblage with *Paratrochamminoides* and *Trochamminoides* has disappeared, but *Recurvoides gerochi* and *R. pseudoregularis* are still common. Within the CIE−interval the agglutinated assemblage is dominated by *Glomospira spp*. Such assemblages, similar to the „Biofacies B“ assemblage or to the „*Glomospira* event“ occur in the Cretaceous and in the Early Eocene of the North Atlantic and Tethys (comp. Kuhnt et al., 1989; Kaminski et al., 1996).

Radiolarians

Occurrences of radiolarians are restricted to the lower part of the section, where they are abundant from samples Mu18a to Mu14 and common in samples Muu2, Mu10, and Mu10d. In the finest grained sieve−residue of sample Mu19, radiolarians are the dominant component. The radiolarians are all spheroidal spumellarians, but are taxonomically indeterminable, since their siliceous skeletons are poorly preserved, due to their replacement by smectite. The abundance of siliceous plankton indicates high nutrient levels in oceanic surface waters in the basal Eocene. A coeval increase in both sedimentation rates and the amounts of terrestrially derived quartz and feldspar suggests that this high primary productivity was the result of enhanced continental run−off. No radiolarians were found further up-section in outcrop 1b.

Figure A1.6 ►
Photograph of outcrop 1b at Untersberg displaying yellowish bentonite layers

Outcrop 1b:
Volcanic ash-layers in the Lower Eocene

Within grey marlstone (calcareous nannoplankton sub−Zone NP10a; planktonic foraminifera Zone E3 – s. Tab.1) thirteen light yellowish layers consisting essentially of smectite were found. These 0.2 cm to 3 cm thick bentonite layers are interpreted as volcanic ashes. No bentonites were found in either the lower part of zone NP9 or in the overlying sub−zone NP10b, which are exposed in other outcrops of the area. The occurrence of bentonites is therefore exclusively restricted to sub−zone NP10a.

Due to their complete conversion to smectitic clay the original chemical composition of the bentonites must have strongly changed. Consequently, only the immobile elements have been used to assess the composition of the original magma (Winchester and Floyd, 1977). The immobile element contents of most of these altered ash layers show very little variation: Nb 28.3 ± 4.7 ppm, Zr 259 ± 104 ppm, Y 25.0 ± 9.5 ppm, and TiO_2 4.82 ± 0.7 wt% (see Fig. 5).

These samples plot in the discrimination diagram of different magma sequences in the field of alkali−basalts. Basaltic ashes are rare in the geological record as the generation of basaltic pyroclastics requires an interaction between basaltic lavas and meteoritic water (see Heister et al., 2001, for a review). Layer M3 (Fig. A1.8) has a totally different composition with highly enriched Nb and Zr, equal Y, and depleted TiO_2 compared to the other bentonites. It is the oldest and thickest layer of the ash−series and plots at the border of trachyte and trachy−andesite.

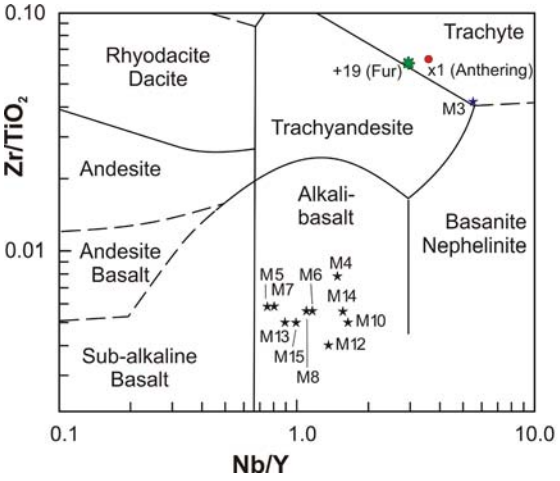

sample	Nb	Zr	Y	TiO_2
M15	28.1	232.8	28.1	47650
M14	33.0	276.9	26.5	51480
M13	28.2	241.6	31.4	49160
M12	26.5	221.4	17.0	54700
M10	31.5	269.9	17.8	55170
M8	25.8	231.8	22.2	43300
M7	24.6	239.1	30.6	42000
M6	28.0	237.8	23.9	44140
M5	25.3	242.5	34.5	42700
M4	31.3	363.0	21.1	46600
M3	121.8	480.6	21.3	11760

All data in ppm.

Figure A1.7 ◄
Magma composition of different ash-layers by means of immobile element distribution (after Winchester and Floyd, 1977). For comparison, sample +19 from the Danish Fur Formation and sample X1, from the Austrian Anthering Formation, are plotted (from Egger et al., 2000).

Figure A1.8 ◄
Photograph showing bentonite layer M3 at Untersberg

The biostratigraphical and geochemical correspondence of these tephras with ashes from the North Sea Basin suggests that these pyroclastic deposits are related to the continental breakup of Europe and Greenland (Egger et al, 2000; Huber et al.,2003; Egger & Brückl, 2006). There, the North Atlantic Igneous Province (NAIP), which is one of the largest basaltic lava accumulations on Earth, formed in the early Paleogene (62 – 53 Ma), prior to and during the continental break-up between Europe and Greenland (Eldholm & Grue 1994; Ritchie & Hitchen 1996; Ross et al. 2005). Beside voluminous flood basalts and associated igneous intrusions, it produced widespread pyroclastic deposits. From the early Eocene Fur Formation in Denmark more than 200 ash-layers of predominantly basaltic composition have been recorded from this explosive volcanic activity (Knox & Morton 1988; Heister et al. 2001). A numbering system for most of these layers was introduced by Bøggild (1918) and is still in use: The upper, closely spaced layers constitute the "positive series", with layers numbered + 1 to + 140 in ascending order. The lower, more widely spaced and generally thinner layers make up the "negative series", and are numbered - 1 to - 39 in descending order.

The paroxysm of this volcanic activity, the positive ash-series, consists of tholeiitic ferrobasaltic layers with the exception of layer + 19. In the immobile element diagram of Floyd and Winchester (1976) this layer plots at the border between trachyte and trachyandesite, whereas more detailed geochemical investigations indicate a rhyolitic composition of the original magma (Huber et al., 2003; Larsen et al. 2003). Some of the ashes of the positive series have also been found at many other sites in Denmark, the North Sea, England, the Goban Spur southwest of Ireland, and the Bay of Biscay (Knox 1984). Based on detailed multi-stratigraphic and geochemical investigations, the most distal equivalents of layer + 19 and 22 other layers have been identified in the Anthering and Untersberg outcrops (Fig. A1.3) of the Austrian Alps near Salzburg (Egger et al. 2000 and 2005; Huber et al. 2003).

It can be assumed that the ash-layers of the NAIP form important correlation horizons for lower Eocene deposits in large areas of Europe. In addition to the Austrian outcrops, reports of lower Eocene basaltic ash layers exist from Switzerland and Poland (Winkler et al. 1985; Waskowska-Oliwa & Lesniak 2002), although stratigraphic and geochemical information from these deposits is insufficient for a detailed correlation.